Journal of the Korean Electrochemical Society
Vol. 7, No. 3, 2004, 131-137

Change of Electrochemical Characteristics Due to the Fe Doping in Lithium Manganese Oxide Electrode

Jeh Beck Ju†, Tae Young Kang, Sung Jin Cho, and Tae Won Sohn
Department of Chemical Engineering, Hongik University, Seoul 72-1, Korea

(Received May 7, 2004 : Accepted June 17, 2004)

Abstract : Sol-gel method which provides better electrochemical and physiochemical properties compared to the solid-state method was used to synthesize the material of $LiFe_yMn_{2-y}O_4$. Fe was substituted to increase the structural stability so that the effects of the substitution amount and sintering temperature were analyzed. XRD was used for the structural analysis of produced material, which in turn, showed the same cubic spinel structure as $LiMn_2O_4$ despite the substitution of Fe^{3+}. During the synthesis of $LiFe_yMn_{2-y}O_4$, as the sintering temperature and the doping amount of Fe(y = 0.05, 0.1, 0.2)were increased, grain growth proceeded which in turn, showed a high crystalline and a large grain size, certain morphology with narrow specific surface area and large pore volume distribution was observed. In order to examine the ability for the practical use of the battery, charge-discharge tests were undertaken. When the substitution amount of Fe^{3+} into $LiMn_2O_4$ increased, the initial discharge capacity showed a tendency to decrease within the region of 3.0~4.2 V, but when charge-discharge processes were repeated, other capacity maintenance properties turned out to be outstanding. In addition, when the sintering temperature was 800~850°C, the initial capacity was small but showed very stable cycle performance. According to EVS(electrochemical voltage spectroscopy) test, $LiFe_yMn_{2-y}O_4$(y = 0, 0.05, 0.1, 0.2) showed two plateau region and the typical peaks of manganese spinel structure when the substitution amount of Fe^{3+} increased, the peak value at about 4.15 V during the charge-discharge process showed a tendency to decrease. From the previous results, the local distortion due to the biphase within the region near 4.15 V during the lithium extraction gave a phase transition to a more suitable single phase. When the transition was derived, the discharge capacity decreased. However the cycle performance showed an outstanding result.

Key words : Lithium manganese oxide, Electrochemical voltage spectroscopy, Capacity fading.

1. Introduction

As the world approaches to the 21st century, miniaturization and minimization of weight for cellular batteries have been accelerated as well as the necessity of mobile electrical power source of the new generation has been emphasized to replace the existing mobile power source such as Ni-Cd battery, from the aspects of higher efficiency, minimized weight and higher energy density. Lithium secondary batteries is expected to be highlighted as the future potable electric power source since it is more outstanding in energy density and many other properties compared to the existing secondary batteries. Among the cathode materials of lithium secondary battery, $LiMn_2O_4$ consists of spinel structure and shows the highest level of operative voltage. Within the spinel structure, 8a tetrahedron and 16c octahedron both share the surface area and configure a three-dimensional (1 × 1) channel which supplies the space for lithium ions to transfer.[1,2] $LiMn_2O_4$ has many advantages compared to the other cathode materials. Since manganese is used as the basic transition metal, it is cheaper in price compared to other cathode materials as well as produces less environmental problems and easy to be synthesized. Moreover, manganese has been already applied for the primary battery so that a lot of information concerning to the recycling of manganese has been known. In addition, in the spinel structure of $LiMn_2O_4$, 75% of metal ions are placed alternately within the oxygen ion layer and the other 25% of metal ions exist within another layer so that it gives an extensive amount of bonding energy which in turn $LiMn_2O_4$ provides ccp configuration to be maintained during lithiation process.[2]

In turn, when it is used as the cathode material of lithium battery, during the process of the insertion and extraction of Li^+ ion between the layers, it undergoes isotropic volume change while maintaining cubic structure which is more stable than stratified structure such as $LiCoO_2$ and $LiNiO_2$ that undergo anisotropic volume change. However, if the average oxidation number of $LiMn_2O_4$ becomes 3.5 or smaller than that, because of CFSE(crystal field stabilization energy), octahedron structure of MnO_6 expands along the direction of Z axis and then Jahn-Teller distortion, the transition into tetragonal structure, occurs.[3]

Phase transition by CFSE propagates to the direction of d orbital function to be stabilized and d^4 compounds which has

†E-mail: jbju@wow.hongik.ac.kr

4 electrons within d orbital starts to change in energy level so that obtains an advantage in energy by the amount of δ. For the case of Mn^{3+} whose electron configuration is d^4, Jahn-Teller distortion undergoes as it did for the previous case. For those kinds of phase transition, it thermodynamically produces a stable phase, but also accompanies 20% of volume expansion that implies as the major element of deteriorating the reversible property of cathode material. If $LiMn_2O_4$ was applied at the 4 V region, the average oxidation number of manganese becomes 3.5 or grater than that within the whole part of charge-discharge process and therefore, it has less possibility of phase transition by Jahn-Teller distortion compared to the 3 V region where the oxidation number changes within the range of 3.5~3.0. However, within the 4 V region, due to the insertion of lithium ions between the layers that happens near the end of its discharge process, reduction of Mn^{4+} proceeds and therefore, the amount of Mn^{3+} that consists of d^4 configuration($t^3_{2g} \cdot e^1_g$) increases so that the average oxidation number becomes approximately 3.5 and phase transition influenced by the Jahn-Teller distortion also occurs.[3,4] There are a few methods of preparing the phase with the oxidation number of Mn equal to or grater than 3.5, but in this experiment, a portion of Mn^{3+} was substituted to Fe^{3+} that consists of d^5 configuration($t^3_{2g} \cdot e^2_g$) so that $LiM_yMn_{2-y}O_4$ (y = 0, 0.05, 0.1, 0.2) was prepared by the citric acid method. The effect of the substitution amount of Fe(y) as well as the variations in physiochemical properties and electrochemical properties due to the sintering temperature were examined to obtain the basic information concerning the preparation of cathode active materials having better reversible and more stabilizing property during the charge-discharge process.

2. Experimental

2.1. Sample preparation

Solid state reaction has been used as one of the most common synthetic methods of $LiMn_2O_4$ and this method is stable for a large scale production but during mixing, considerable amount of impurities inflow from ball-mill and as it only undertakes a simple mechanical mixing, obtaining evenly distributed phase is rare and is also hard to control the grain size of powder so that the sintering efficiency gets decreased. However, the citric acid method, one of the liquid state methods, is easy to control the composition rate and gets less amount of inflow impurities and even the grain size is adjustable in microscopic level so that possibly obtains the sample powder with large surface area and evenly distributed grains, subsequently a lot of researches proceeded so far. First of all, mixing $LiNO_3$ and $Fe(NO_3)_3 \cdot 9H_20$ in stoichiometric ratio by using $Mn(NO_3)_2 \cdot 6H_2O$ and then dissolve it and mixing it for 2 hrs. Substitute citric acid for the mixed solution with a certain molar ratio and eliminate moisture using rotary evaporator and then dry the mixture at the approximate temperature range of 70~80°C so that the mixture turns into viscous gel state. In turn, the organic substances was eliminated by heat treatment at the temperature of 250°C for 35 hrs. After the heat treatment finishes, grinding process undergoes and in turn sintered it under air circumstance for 8 hrs with an applied temperature of 700~850°C. Finally active materials were produced after a final slow cooling step.

2.2. Physiochemical characterization

A research within the range of 2θ: 10° ~80° and 2°/min inserting speed used X-ray Diffraction (Cukα radiation, 40KV, MAC Science Japan) to analyze the structure of the produced sample. Rietvield refinement analysis was proceeded using X-ray diffraction results to find the lattice constant of $LiFe_yMn_{2-y}O_4$. Specific surface area was measured by BET method, using nitrogen gas, and surface area analyzer (Micromeritics Co, ASAP-2010) was used for this measurement. The dimensional change and morphology were measured using field emission SEM(XL-50) from Phillips. Porosimeter(Micromeritics Co, porosizer 9320) was used to observe the pore volume affected from the substituted amount of Fe^{3+}.

2.3. Cell assembly

Active materials of cathode produced within aluminum ex-metal collector, acetylene black and binder(PVDF) were mixed together with suitable weight ratios and then, they got dissolved in acetone so that formed slurry state mixture which subsequently dipped and dried sufficiently. After pressing the sufficiently dried electrode, dry it again for 24 hrs in vacuum. Copper ex-metal collector was applied with lithium metal pressed on it. Polypropylene film and 1 M $LiPF_6$ EC/DMC (1:1) were used as a separated membrane and an electrolyte respectively. For the construction of cell, vacuum vinyl was used and all electrochemical experiments were performed at room temperature in a glove box filled with high purity argon gas(99.999%).

3. Results and Discussion

3.1. Crystal structure and microstructure

In Fig. 1, it showed XRD pattern of the sample prepared by sintering gel precursor at the temperature of 700°C for 8 hrs under air condition that is for observing the changes of

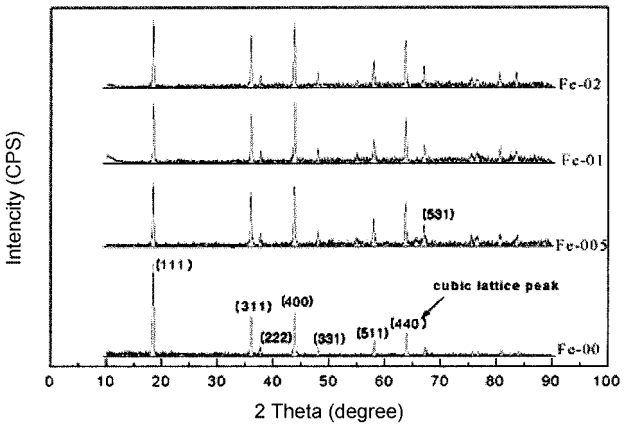

Fig. 1. X-ray diffraction patterns of $LiFe_yMn_{2-y}O_4$.

crystalline due to the substitution amount of Fe^{3+}. It had a high level of crystalline by the sintering at the temperature of 700°C and also showed little impurities. When Fe^{3+} was substituted to $LiMn_2O_4$, the intensity of the peak(111) that is corresponding to the value of displacement between planes, d100 was a bit low but it could be observed that the intensity of cubic spinel peak(440) was increased.

In Fig. 2, samples same in Fig. 1, has been processed by rietvield-refinement analysis and represented lattice constant **a**, by using cubic lattice peak(440) of cubic spine $LiFe_yMn_{2-y}O_4$ (y = 0.05, 0.1, 0.2) powder due to the substitution amount of Fe^{3+}. Lattice constant **a**, increased linearly with the substitution amount of Fe^{3+}, and it is because of the reduction of the oxidation number of manganese cation as well as the fact that Mn^{4+} with a relatively small ionic radius distributed extensively in to the lattice by substituting a part of Mn^{3+} with Fe^{3+}.[5] For Tarascons material made from Bellcore company, the **a** value of $LiMn_2O_4$ sample should be smaller than 8.23 to reduce its oxygen vacancy so that maintains a stable structure and it shows stable discharge properties for more than 200 cycles.[6] In this study, by setting on the basis of sintering temperature at 700°C, **a** values due to the substitution amount of Fe were 8.21(y=0, $LiMn_2O_4$), 8.222 (y=0.05), 8.229 (y=0.1) and 8.245(y=0.2), respectively. When the materials have **a** values of 8.222(y=0.05) and 8.229(y=0.1) which are lower than 8.23, they showed practically outstanding discharge properties.

Fig. 3 represents specific surface area dependency of $LiFe_yMn_{2-y}O_4$ powder due to the substitution amount of Fe^{3+} and sintering temperature. As the Fe^{3+} substitution amount and sintering temperature(700~850°C) increased, the surface area of sample decreased linearly that is because of the grain growth caused by sintering. In this experiment, as the substitution amount of Fe increased, the surface area decreased more significantly compared to the pure $LiMn_2O_4$. However, when Fe(y=0.05 and 0.1) were substituted, their surface area were analogous each other at 700°C, and the variation of the surface area occurred due to the sintering temperature. For the case of $LiMn_2O_4$ with no Fe substitution, it showed the surface areas as 5.36 m^2/g and 4.87 m^2/g at 700°C and 750°C respectively, but also showed 3.58 m^2/g and 3.12 m^2/g at

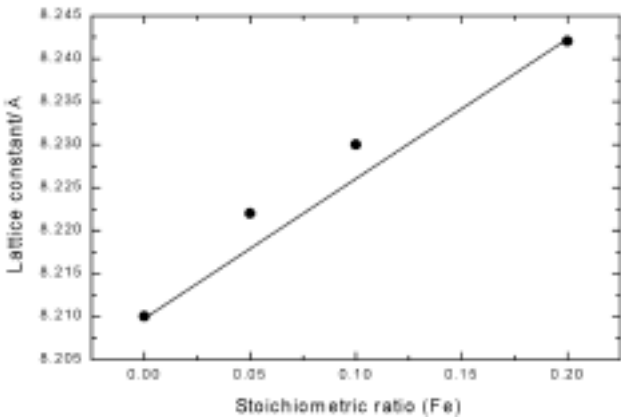

Fig. 2. Effect of the amount of Fe on the lattice constant.

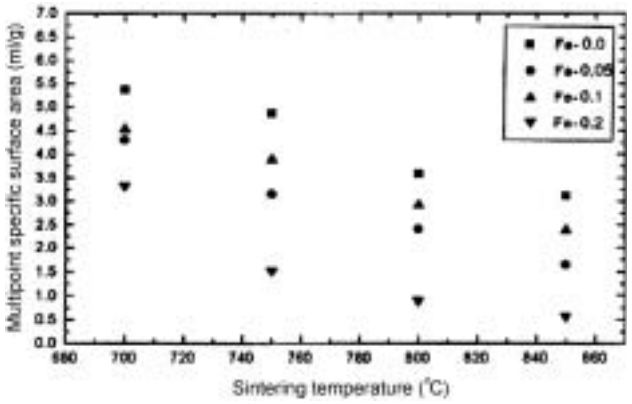

Fig. 3. Multipoint specific surface area of $LiFe_yMn_{2-y}O_4$ powders prepared with various sintering temperatures.

800°C and 850°C respectively which are similar with the surface area of commercially selling $LiMn_2O_4$, 3 m^2/g. When y=0.05, it showed 4.3 m^2/g at 700°C and, when y=0.1, it also approached to 3 m^2/g between 750°C and 800°C, and when y=0.2, it represented 3.3 m^2/g at 700°C.

From Fig. 4(a) to Fig. 4(d), it showed the grain shape of $LiFe_yMn_{2-y}O_4$ due to the substitution amount of Fe (y=0, 0.05, 0.1, 0.2) by suing field emission SEM. As can be seen in the figure, for the cases of no substitution as well as y=0.05 and 0.1, grains were distributed relatively even, but for the case of y=0.2, grains bounding together and formed a macro-grain. Fig. 5 shows the distribution of air holes due to the substitution amount of Fe. As seen from the SEM morphology, pore volume showed a tendency to increase as the Fe substitution amount increased.

3.2. Charge-discharge properties

Charge discharge experiments were measured by a cyclic tester (Won-A tech company, WBCS-3000) and for charge-discharge process, the experiments proceeded with current adjusted to 1 mA/cm^2 and applied voltage of 3.0 V ~ 4.2 V that was undertaken up to 1~50 cycles. From the discharge curve, the sample showed two plateau regions which are known as typical property of manganese spinel structure. During the lithium inserting process, in the mechanism used, there are two equilibrium systems that are λ-MnO_2 becoming $Li_{0.5}Mn_2O_4$ and $Li_{0.5}Mn_2O_4$ becoming $LiMn_2O_4$, which in turn shows two transition plateau regions. Fig. 6(a) is the discharge curve of $LiMn_2O_4$. The initial discharge capacity was 110 mAh/g which is corresponding to 74.2% of the theoretical capacity of $LiMn_2O_4$, 148.21 mAh/g. After 20 cycles, it showed 92 mAh/g and after 30 cycles it became 75 mAh/g that is a large capacity fading of 31.8%.

Fig. 6(b) is the discharge curve of $LiFe_{0.05}Mn_{1.95}O_4$. Since, the substitution amount of Fe was very small, the initial discharge capacity was 110 mAh/g that is the same as $LiMn_2O_4$. However, after 30 cycles, it showed 100 mAh/g, 9% of capacity fading, and after 50 cycles, it became 94 mAh/g which shows a serious capacity fading difference compared to $LiMn_2O_4$. Fig. 6(c) is the discharge curve of $LiFe_{0.1}Mn_{1.9}O_4$. The initial discharge capacity was 102 mAh/g that is smaller than $LiMn_2O_4$

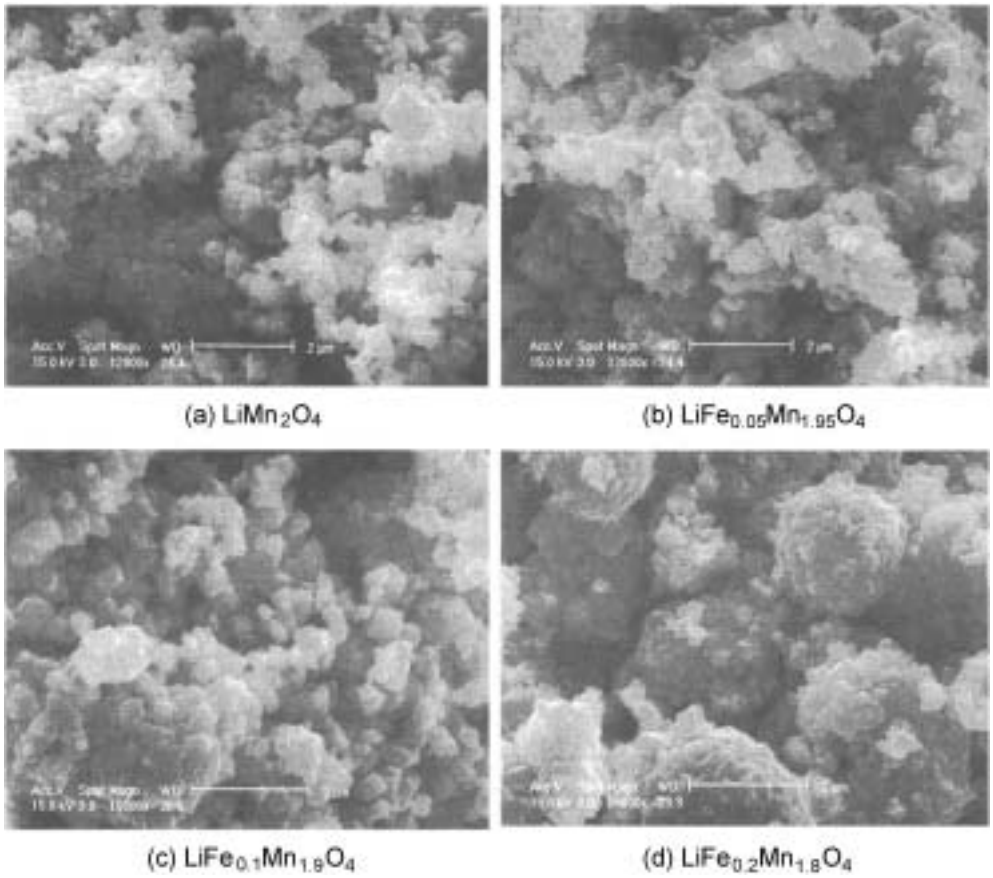

Fig. 4. SEM images for various electrode materials.

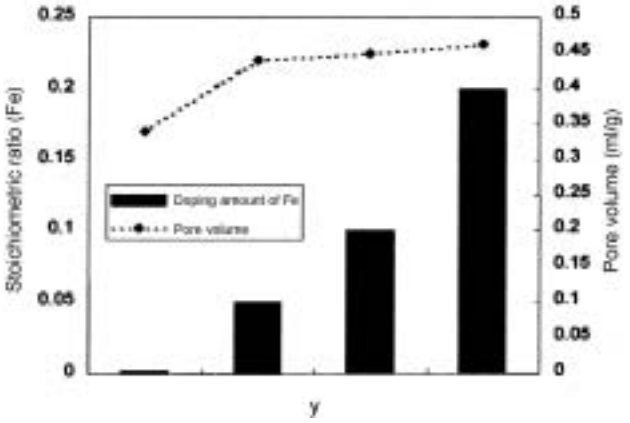

Fig. 5. Total pore volume of $LiFe_yMn_{2-y}O_4$ with various stoichiometric ratios(Fe).

and $LiFe_{0.05}Mn_{1.95}O_4$, but after 20 cycles, the discharge capacity reduced to 92 mAh/g and then to 90 mAh/g after 30 cycles, which are 9.8% and 11.96% of capacity fading, respectively.

Fig. 6(d) is the discharge curve of $LiFe_{0.2}Mn_{1.8}O_4$. The initial discharge capacity was 97 mAh/g, the smallest among the results. The discharged capacity reduced to 87 mAh/g after 20 cycles and became 81mAh/g after 30 cycles which are 9.4% and 15.6% of capacity fading, respectively.

Fig. 7 shows the discharge capacity up to 30 cycles due to the Fe substitution. According to these results, as the substitution amount of Fe increased, although the initial discharge capacity was small, the cycle properties came out outstandingly. The phenomenon of reduction of the initial discharge capacity due to the increase of Fe substitution is explained as following reasons. During the charge-discharge of $LiMn_2O_4$, variations in charge capacity occur due to the oxidation-reduction reaction of $Mn^{4+} \leftrightarrow Mn^{3+}$ as lithium insertion/extraction. Fig. 8 shows the effect of its sintering temperature on the discharge capacity of $LiFe_{0.05}Mn_{1.95}O_4$. While it was sintered at 700°C and 750°C, the initial discharge capacity as well as the capacity fading was considerably large. However, when it was sintered at 800°C and 850°C, the initial discharge capacity was low but the capacity fading was less than 10%.

3.3. Electrochemical voltage spectroscopy

EVS is the most recently innovated electrochemical analytic method and it integrates current against time so that evaluates the electrical current consumed for the given reaction and the variations in the amount of current within the transition region of current transferring reaction are represented as peaks. In Fig. 9(a)~9(d), it shows the results of EVS experiments accomplished within the transition insertion range of $LiFe_yMn_{2-y}O_4$ ($y = 0, 0.05, 0.1, 0.2$) in 3.0 V ~ 4.6 V.

As seen in the figure, for the case of $LiFe_yMn_{2-y}O_4$ spinel

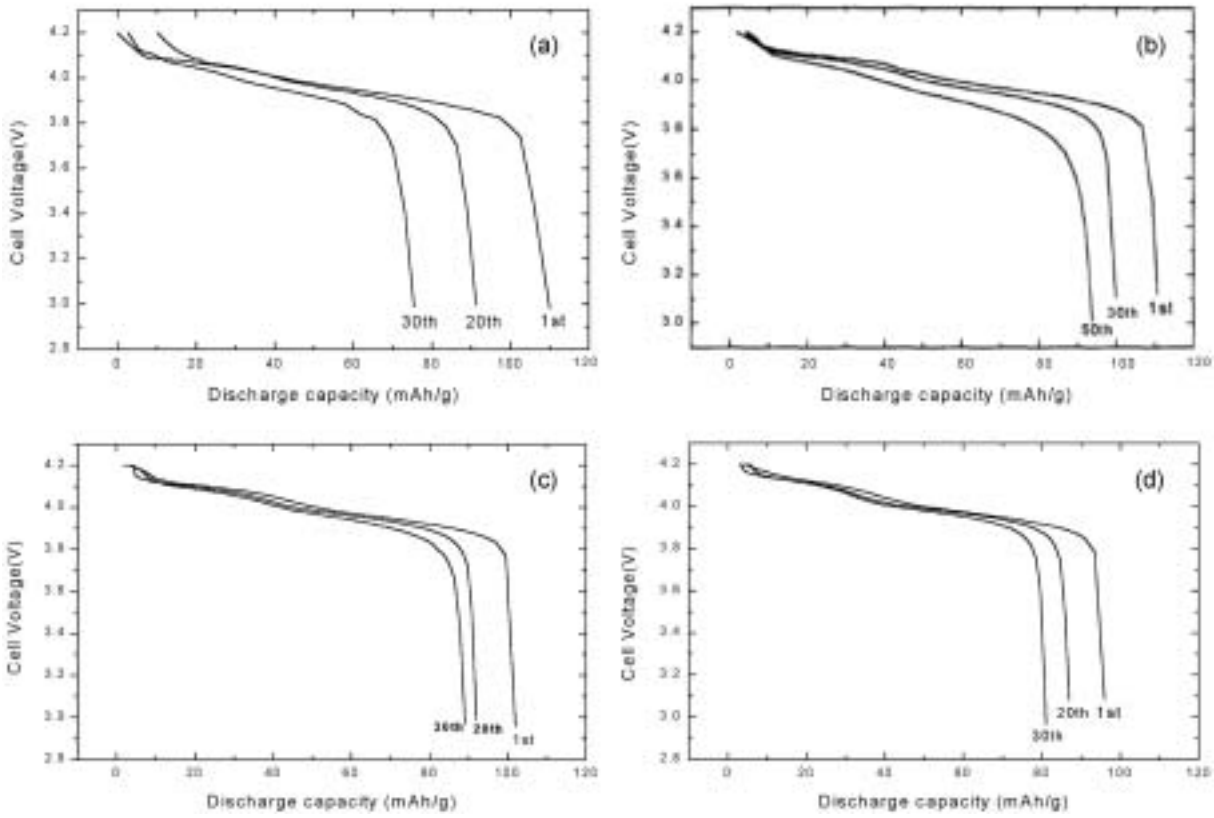

Fig. 6. (a) The 1st, 20th and 30th discharge curves performed at a current rate of C/3 for $LiMn_2O_4$. (b) The 1st, 30th and 50th discharge curves performed at a current rate of C/3 for $LiFe_{0.05}Mn_{1.95}O_4$. (c) The 1st, 20th and 30th discharge curves performed at a current rate of C/3 for $LiFe_{0.1}Mn_{1.9}O_4$. (d) The 1st, 20th and 30th discharge curves performed at a current rate of C/3 for $LiFe_{0.2}Mn_{1.8}O_4$.

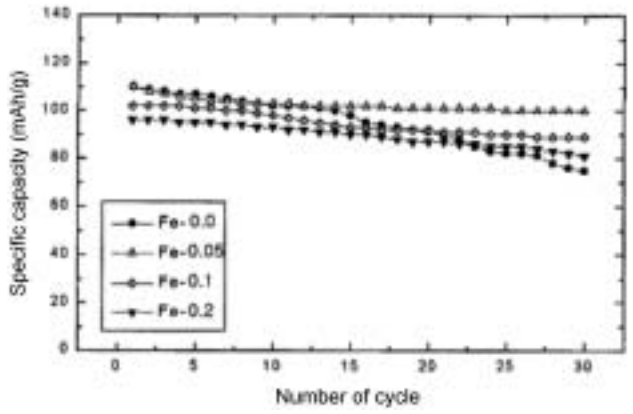

Fig. 7. Variation of specific capacities with number of cycle for $LiFe_yMn_{2-y}O_4$.

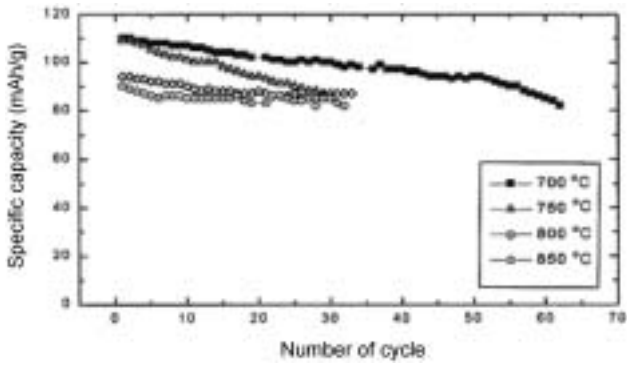

Fig. 8. Variation of specific capacities with the change of sintering temperature for $LiFe_{0.05}Mn_{1.95}O_4$.

compound, two peaks occur at 4.0 V and 4.15 V during charge-discharge. According to Farringtons report,[7] those kinds of peaks mentioned previously can be classified very clearly into the compounds of stoichiometric ratio spinel structure as the heat treatment temperature increases. When manganese ion is substituted with the other kind of ion, the peak intensity decreases in turn as the substitution amount increases and finally the peaks cannot be differentiated with the other regions. The previous phenomenon is affected from the structural variations of spinel.[7] Therefore, if the considerable variation in discharge capacity of $LiMn_2O_4$ is assumed as the unique property of coexistence of two phases, by watching the changes of the second peak near 4.15 V which is known as the co-existence region of two peaks, it clearly shows that the peak size gradually decreases as the substitution amount of Fe increases so that the potential difference between oxidation peak and reduction peak also gets decreased gradually. This implies that as the Fe substitution amount increases, it accompanies a variation in the amount of insertion /extraction of lithium ions, but structurally more stable single phase is induced and the diffusion of lithium ion become easier.

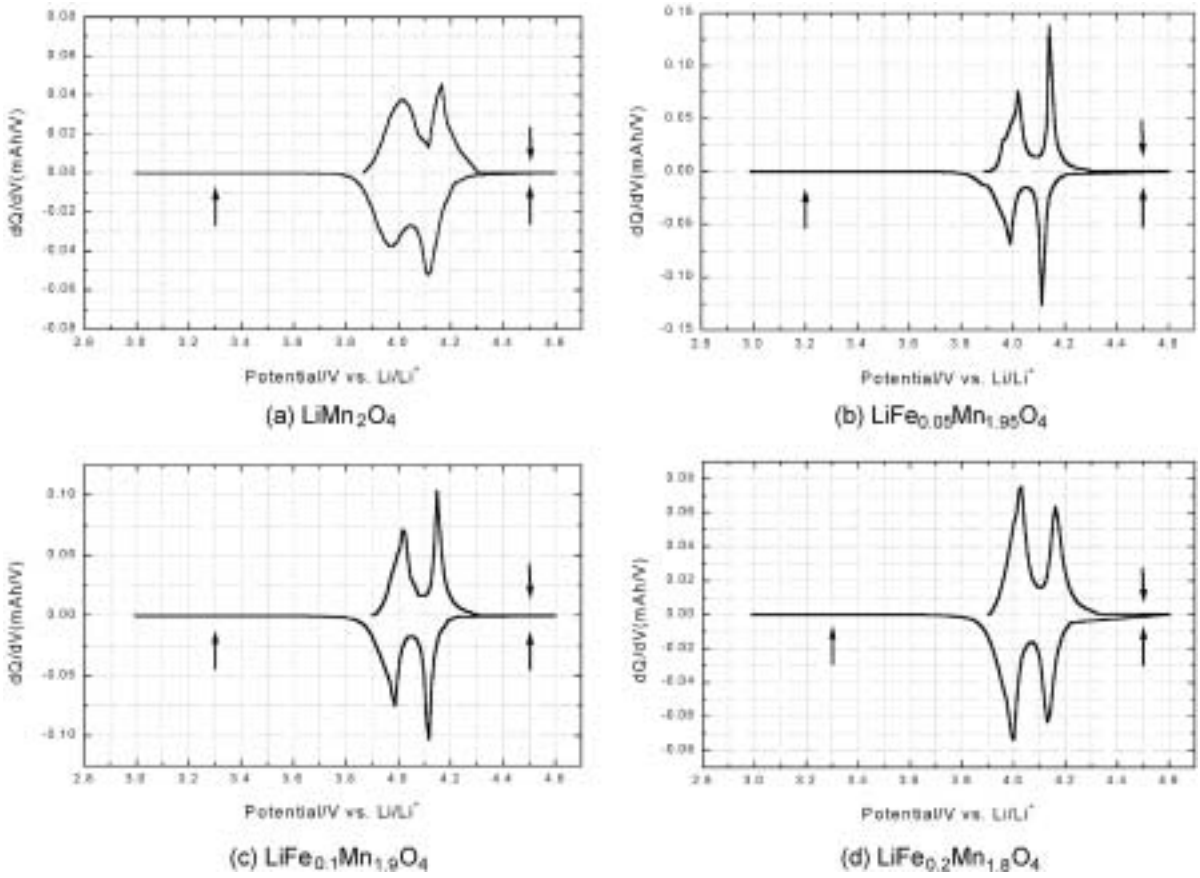

Fig. 9. EVS results for the first cycle with $LiFe_yMn_{2-y}O_4$ in the voltage range from 3.0 to 4.6 V.

Therefore, according to those phenomena, for the case of $LiFe_yMn_{2-y}O_4$ substituted with Fe, the discharge capacity is smaller than $LiMn_2O_4$ but from the aspect of electrode property that is comparing the cycle performance, $LiFe_yMn_{2-y}O_4$ turned out to be very outstanding. In addition, the existence of the two peaks that are a 3.3 V(vs. Li/Li^+) peak that appears during discharge due to the oxygen deficiency[8] and the reversible peak of oxidation/reduction at 4.5 V(vs. Li/Li^+) due to the state-changing phenomenon of cation[6] was examined. In 1 M $LiPF_6$ EC:DMC (1 : 1 v/v) electrolyte known as stable up to 5 V (vs. Li/Li^+) and no peaks were found at 3.3 V and 4.5 V. From the results, $LiFe_yMn_{2-y}O_4$ substituted with Fe can be a method that can compensate both the oxygen deficiency problem and the capacity fading due to the state-changing phenomenon of cation.

4. Conclusion

$LiFe_yMn_{2-y}O_4$ (y = 0, 0.05, 0.1, 0.2) was synthesized using citric method which gives better physiochemical and electrochemical properties than solid state method and Fe^{3+} was substituted so that the effects of substitution amount of Fe^{3+} and sintering temperature were analyzed to enhance the structural stability. The sintering temperature was considerably high for the case of $LiFe_yMn_{2-y}O_4$ synthesis and as the substitution amount of Fe(y = 0.05, 0.1, 0.2) increased, crystalline and grain size were high due to the grain growth so that morphology having small surface area and large air hole distribution could be observed. For the case of $LiFe_yMn_{2-y}O_4$ synthesis, when Fe (y = 0.05 and 0.1) were substituted, it could maintain the surface area similar to the one of commercial powder, and the powder sintered at 800°C had more evenly distributed grain size and shape than the one sintered at 700°C. As the substitution amount of Fe^{3+} on to $LiMn_2O_4$ increased, the initial discharge capacity showed a tendency to decrease near 3.0 V ~ 4.0 V, but as charge-discharge repeated, other capacity maintaining properties were very satisfied. For the case of $LiFe_{0.05}Mn_{1.95}O_4$ synthesis, initial capacity and capacity fading were considerably large when the sintering temperature was 700~750°C but when the sintering temperature was 800~850°C, although the initial capacity was small, the cycle property was very stable. For all of electrodes of $LiFe_yMn_{2-y}O_4$ (y = 0, 0.05, 0.1, 0.2), two transition plateau regions which is known as the typical behavior of manganese spinel structure were obtained and as the substitution amount of Fe^{3+} increased, the peak value within 4.15 V region during the charge-discharge showed a tendency to decrease. This may be explained that the local distortion during the lithium extraction due to bi-phase generating near 4.15 V proceeds induced phase transition to single phase so that affects on the charge-discharge property.

Acknowledgements

The authors acknowledge the financial supports by 2003 Hongik University Research Fund.

References

1. N. Kumagal, T. Fujiwara. and K. Tanno, *J. Electrochem. Soc*., **143**, 1007 (1996).
2. R.J. Gummow and M.M. Thackeray, *J. Electrochem. Soc*., **141**, 1178 (1994).
3. T. Ohzuku, M. Kitagawa. and T. Hirai, *J. Electrochem. Soc*., **137**, 769 (1990).
4. T. Ohzuku, J. Kato, K. Sawai, and T.Hirai, *J. Electrochem. Soc*., **128**, 2556 (1991).
5. C. Masquelier, M. Tabuchi, K. Ado, R. Kanno, Y. Kobayashi, Y. Maki, O. Nakamurra, and B. Goodenough, *J. Solid State Chem*. **123**, 255 (1996).
6. D. Guyomard and J. M. Tarascon, Solid State Ionics. **69**, 222 (1994).
7. W. Liu. K, Kowal and G. C. Farrington, *J. Electrochem. Soc*., **143**, 3590 (1996).
8. W. Li, J. N. Reimer, and J. RDahn, Solid State Ionics., **67**, 123 (1993).